Special Feature: Power Semiconductor Devices

Research Report

Imaging of Current Collapse and Degradation in Schottky Gate AlGaN/GaN HEMT by Electric Field-induced Optical Second-harmonic Generation Measurement

Takashi Katsuno, Takaaki Manaka, Tsuyosihi Ishikawa, Hiroyuki Ueda, Tsutomu Uesugi and Mitsumasa Iwamoto

Report received on Aug. 18, 2015

ABSTRACT Two-dimensional (2D) imaging of current collapse and degradation in a Schottky gate AlGaN/GaN high electron mobility transistor (HEMT) device was achieved through electric field-induced optical second-harmonic generation (EFISHG) measurement. EFISHG measurement can detect the electric field produced by the carriers trapped at the on-state of the device, which leads to the current collapse. Immediately after (e.g. 1, 100 or 800 μs) completion of the drain-stress voltage (200 V) in the off-state, the second-harmonic (SH) signals appeared within 2 μm from the gate edge on the drain electrode. This signal location corresponds to the location by the well-known virtual gate model of current collapse. In addition, a strong SH signal was observed before destruction at the location of a small defect in the gate edge upon application of a high drain stress voltage (300 V). EFISHG measurement is also effective for analysis of the degradation and destruction mechanisms in AlGaN/GaN HEMTs.

KEYWORDS Power Device, GaN, Current Collapse, Reliability, Degradation, EFISHG, Imaging

1. Introduction

Gallium nitride (GaN) is an excellent candidate for electronic power devices due to its superior properties, such as high breakdown voltage, high thermal resistance, and low on-resistance.(1,2) In particular, the AlGaN/GaN high electron mobility transistor (HEMT), which utilizes high-density two-dimensional electron gas (2DEG), has received considerable attention as a switching device for next generation power conversion systems.

However, AlGaN/GaN HEMTs have serious problems, one of which is the reduction of drain current at the on-state after the application of drain voltage stress in the off-state; this phenomenon is referred to as current collapse.(3-10) Device performance, such as the output power and the switching characteristics of AlGaN/GaN HEMTs, are limited due to current collapse. Current collapse is generally caused by the charges trapped at the AlGaN barrier surface, AlGaN layer, AlGaN/GaN interface, and GaN bulk.(11-13) Trapped charge carriers are emitted from the trap sites with several time constants τ, and the drain current is recoverable in time.

Kelvin force microscopy (KFM) is often used to investigate the distribution of trapped carriers by measuring the surface potential on AlGaN/GaN HEMT devices.(14-17) High speed switching in AlGaN/GaN HEMTs is required to realize the downsizing of conversion systems; therefore, it is important to investigate the current collapse by imaging immediately after the transition time from the off-state to the on-state. Observation of the trapped charge distribution is required immediately (e.g. 1 μs) after completion of the drain stress-voltage; however, it is difficult to record the surface potential of the device due to the scan speed limitations of the cantilever. Therefore, there is no adequate method to detect the trapped charge distribution in AlGaN/GaN HEMT devices with sub-second resolution after completion of the drain-stress voltage in the off-state.

On the other hand, degradation proceeds at the gate edge on the drain side, due to the mechanical strain induced by a high electric field,(18-22) and an improved observation method of the degradation locations is an effective approach to improve the reliability of these devices. Changes in the surface morphology and oxide particles are often observed along the gate edge of stressed samples.(23,24) Electroluminescence (EL) and photoluminescence (PL) studies have been widely used to investigate the appearance of degradation-related hot spots in AlGaN/GaN HEMTs.[25-28] While the degradation of such devices under off-state conditions is clearly affected by the electric field, it is still necessary to directly observe the electric field distribution in a device.

The traps produced by degradation are also associated with current collapse, which changes the electric field distribution induced by the degradation. Therefore, the current collapse and degradation imaging of AlGaN/GaN HEMTs is important and a method for direct observation of the electric field may be useful to detect the degradation points clearly with high sensitivity.

Electric field-induced optical second-harmonic generation (EFISHG) measurements enable the direct probing of electric fields in organic devices; therefore, this technique represents a very useful means to investigate fundamental processes such as carrier injection and transport.[29-31] In addition, this method makes it possible to acquire information concerning the electric field with a very fine time resolution, because a pulsed laser is used. Furthermore, two-dimensional (2D) imaging can be performed simultaneously with trigger delay measurements. Thus, the advantages of EFISHG measurement are dynamic measurement with high speed and 2D imaging. The weak electric field caused by the trapped charges, which leads to current collapse, may be detected as a second-harmonic (SH) signal at the on-state immediately after application of a high voltage at the off-state. In addition, it is expected that the degradation points of AlGaN/GaN HEMT devices in the off-state may be readily identified using this technique. In this paper, the 2D imaging of current collapse and degradation in AlGaN/GaN HEMT device was investigated using EFISHG measurements.

2. Experimental Method

2. 1 EFISHG Measurement for Current Collapse and Degradation Imaging

Figure 1 shows schematic diagram of the setup for EFISHG measurement. The primary beam from a Ti:sapphire laser (λ = 1000 nm, femtosecond pulse width) passes through a polarizer, a SH-cut filter, and an objective lens (Mitsutoyo, M Plan Apo SL20X, N.A. = 0.28, W.D. = 30.5 mm) before being irradiated onto the sample.[32] The spot size on the sample is about 100 µmϕ. Drain and gate pulse voltages were applied to the sample using a function generator (NF Corp., WF1974). The drain voltage was amplified using an amplifier (Turtle Corp., T-HVA02). SH signals were induced by the light and the applied voltage. The wavelength of the SH signal is λ = 500 nm. The SH signal intensity $I(2\omega)$ is expressed as follows:

$$I(2\omega) \propto |\chi^{(3)}_{xxxx}(2\omega; 0, \omega, \omega)E_x(0)E_x(\omega)E_x(\omega)|^2, \quad (1)$$

where $\chi^{(3)}_{xxxx}(2\omega; 0, \omega, \omega)$ represents the third order nonlinear optical susceptibility, and $E_x(0)$ and $E_x(\omega)$ represent the static local electric field and the electric field of the incident light, respectively. The SH signals are detected only in the drain-source direction due to the use of polarizer located behind the Ti:sapphire laser.

In the measurement of the off-state, $E_x(0)$ is the ratio of the applied drain voltage V_d, and the depletion layer d ($E_x(0) = V_d/d$), in the equation, and the SH signals are largely induced. On the other hand, in the measurement of the on-state, $E_x(0)$ is equivalent to the electric field generated only by the trapped charge carriers, because the applied drain and gate voltages were 0 V under this measurement condition. SH signals were filtered by a fundamental-cut filter to remove the primary beam, and were detected by a

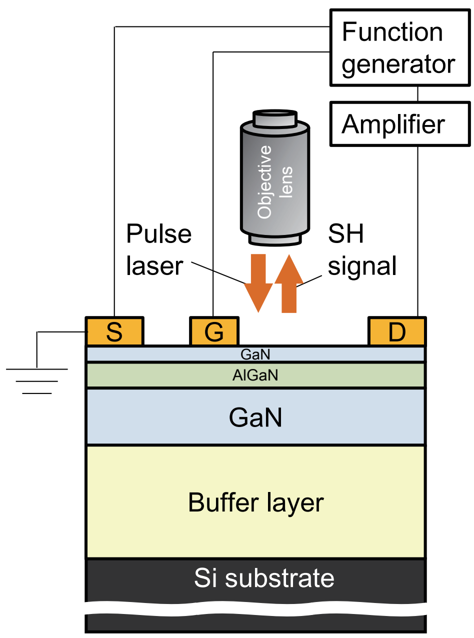

Fig. 1 Schematic diagram of the setup for the EFISHG measurement and cross-sectional diagram of AlGaN/GaN HEMT device.

cooled charge-coupled device (CCD) camera (Andor Technology: DU420-BV). One pixel of the CCD image corresponds to 0.5 × 0.5 μm^2 area. $\chi^{(3)}_{xxxx}(2\omega; 0, \omega, \omega)$ for the GaN material is discussed elsewhere.(33,34) $E_x(\omega)$ is dependent on the laser intensity incident on the sample.

Figure 2 shows timing charts for the pulse laser, and the applied drain and gate voltages in the AlGaN/GaN HEMT device to obtain SH signals under device operation. This device is a normally-on type, and the gate voltage was applied at –5 V to realize the off-state. For conditions (i) and (ii), the pulse laser was irradiated at the on-state and at the off-state, respectively. The timing of condition (i) is to achieve current collapse imaging. The pulse width of the drain and gate voltages is 130 μs. To prevent device destruction during the measurement, the time of the applied gate voltage is slightly longer than that of the drain voltage (ca. 0.1 μs).

For condition (i), the time dependence of the trapped charge distribution is investigated by changing the time delay of the pulse laser (1, 100 or 800 μs) from the end of the applied drain stress voltage (200 V). It is considered that the SH signals are dependent on the time, similar to the dependence of $R_{on}A$, as shown in Fig. 2 (bottom panel). The repetition rate of the pulse laser is 1 kHz and the event duration is 1 ms. The SH signals produced by a single pulse laser may be weakly induced and are integrated for 5 min to clearly visualize the 2D image of the electric field distribution in the AlGaN/GaN HEMT device.

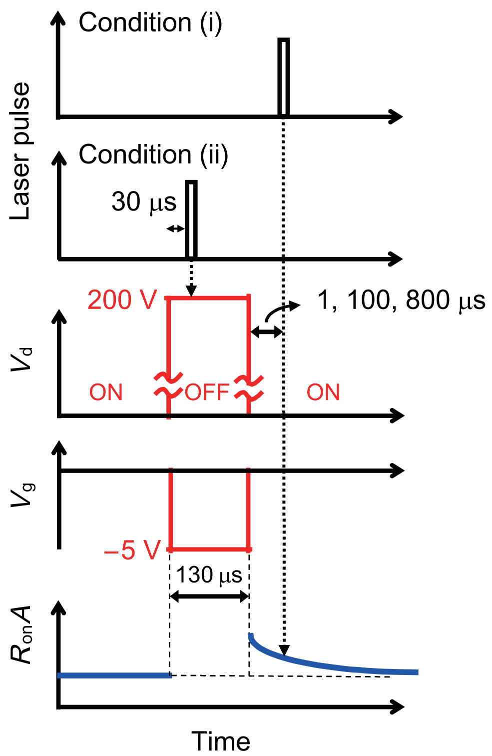

Fig. 2 Timing chart for the pulse laser, and the drain and gate voltages in the device during EFISHG measurement.

For condition (ii), the pulse laser was irradiated at 30 μs after the applied voltage to investigate the electric field distribution in the device at the off-state. The drain voltages were applied at 100, 200 and 300 V with the device in the off-state during the EFISHG measurements. In addition, the device was stressed by the application of 200 V for 1 h in the off-state prior to the condition (ii) SHG measurements. The SHG measurements with condition (ii) were thus conducted using a stressed sample.

2. 2 Device Structure

Schottky gate AlGaN/GaN HEMT devices were used in these experiments. The AlGaN/GaN HEMT device was fabricated on an AlGaN/GaN heterostructure grown on a silicon substrate. The thickness of the AlGaN and GaN layers were 20 nm and 1.6 μm, respectively. A 2 nm thick GaN cap layer was deposited on the AlGaN layer. The Al content in AlGaN is 0.20. Ti/Al layers used as source and drain electrodes were deposited and annealed at 650°C for 5 min in a N_2 atmosphere to ensure the formation of an ohmic contact. Ni was used as a Schottky gate metal. The gate-source length L_{GS}, gate length L_G, gate-drain length L_{GD}, and gate width W_G were 5, 5, 15 and 100 μm, respectively. No passivation layer was used in this device, based on the assumption that the specific on-resistance $R_{on}A$ is large at the on-state of the device immediately after completion of the drain-stress voltage in the off-state.(35) **Figure 3** shows the V_g-I_d characteristics of the device with a drain voltage of 1 V. The threshold voltage V_{th} was –3.5 V, and the normally-on operation was confirmed. The static $R_{on}A$ measured at I_d = 5 mA and V_g = 0 V was 8 mΩ cm^2.

2. 3 Current Collapse Measurement (Time Dependence of $R_{on}A$)

The impact of current collapse was defined as $R_{on}A$. As a method to measure the time dependence of $R_{on}A$

from short to long time at the on-state of the device after the end of the applied drain voltage, the AlGaN/GaN HEMT device and load resistance were connected in series. The drain stress voltage was applied 200 V for 10 s at the off-state. The value between the drain and source voltage V_{DS} of the device was read using an oscilloscope. The operation point of the device was determined by the value of the load resistance (100 kΩ) in the V_g-I_d characteristics, and the on-state drain current I_d, was 2 mA at V_g = 0 V at the on-state. After the end of the applied drain stress at the off-state, the drain voltages V_{DS} from 1 µs to 40 s at the on-state of the device were measured and $R_{on}A$ was calculated.

3. Results and Discussion

3. 1 Current Collapse Imaging

Figure 4 shows an optical microscopy image of the AlGaN/GaN HEMT device surface and SH signals observed at 1, 100 and 800 µs under condition (i). SH signals are observed at the gate edge on the drain side and are extended almost uniformly from the gate edge. **Figure 5** shows the distribution of SH signals obtained from Fig. 4 (condition (ii) is discussed later.). The SH signal intensity is the strongest at the gate edge and decreases with the distance in the direction from the gate edge to the drain. The distribution of SH signals corresponds to the results of KFM measurements.(14-17)

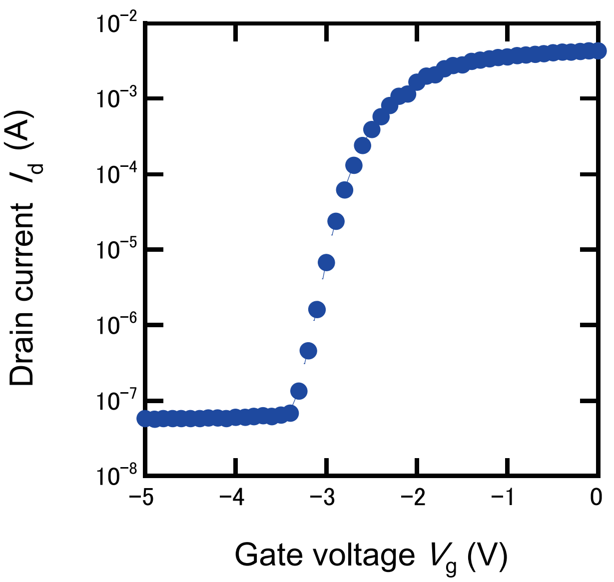

Fig. 3 V_g-I_d characteristics for the AlGaN/GaN HEMT device. V_d was applied at 1 V.

The SH signal intensity becomes weak with an increase in the time, although the signal location is almost 2 µm from the gate edge. In the principle of EFISHG, the generation of an SH signal means that an electric field is present on the device. Under condition (i), both V_g and V_d were applied at 0 V at the on-state in the device, and the SH signals would originate from the trapped charges induced by the drain stress voltage at the off-state in the device.

Figure 6 shows the time dependence of $R_{on}A$ and the SH intensity at the on-state of the AlGaN/GaN HEMT device after the end of the drain voltage at 200 V. $R_{on}A$ is gradually decreased from 1000 mΩ cm^2 at 1 µs to 10 mΩ cm^2 at 40 s, while the SH intensity also decreases with time. $R_{on}A$ and the SH intensity have similar tendencies, where the SH signals indicate that the electric field is created by the trapped charge, which leads to current collapse. The reduction of the SH signal intensity with time is considered to result in carrier emission from the trap sites at the SH signal region (2 µm from the gate edge). The virtual gate model explains the current collapse phenomenon of the AlGaN/GaN HEMT.(36,37) The model shows that the cause of current collapse is the charging up of a second virtual gate that is physically located in the gate-drain access region. Surface states in the vicinity of the gate trap electrons act as a negatively charged virtual gate, due to the large bias voltages present on the device. The visualization of trapped carriers, which leads to current collapse, at the gate edge of the drain electrode was confirmed by the results.

SH signals consist of charges trapped at the AlGaN barrier, AlGaN/GaN interface, and GaN bulk layer in this experiment, because the resolution of the depth direction is about 50 µm due to the use of the objective lens with a low numerical aperture (NA). In previous work,(35) the $R_{on}A$ was significantly reduced when a p-GaN gate GaN HEMT device was covered with a passivation layer. This indicates that the SH signals may originate mainly from the AlGaN barrier only in a device without a passivation layer. The origin of the SH signals in the depth direction will be shown in the next study.

3. 2 Degradation Imaging

Figure 7 shows an optical microscopy image of the AlGaN/GaN HEMT device surface and SH signals observed upon application of 100, 200 and

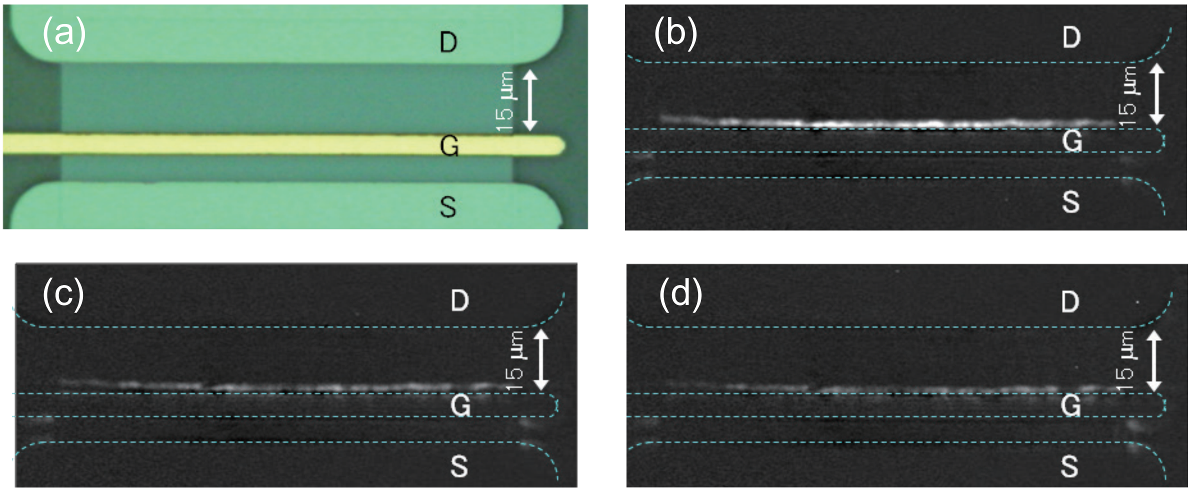

Fig. 4 (a) Optical microscopy image of the AlGaN/GaN HEMT device surface, and (b)-(d) SH signals obtained at 1, 100 and 800 μs after completion of the drain voltage, respectively.

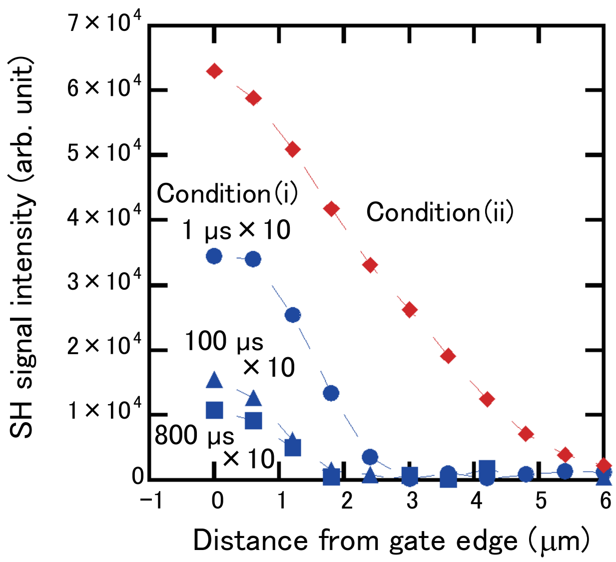

Fig. 5 SH signal distribution for conditions (i) and (ii).

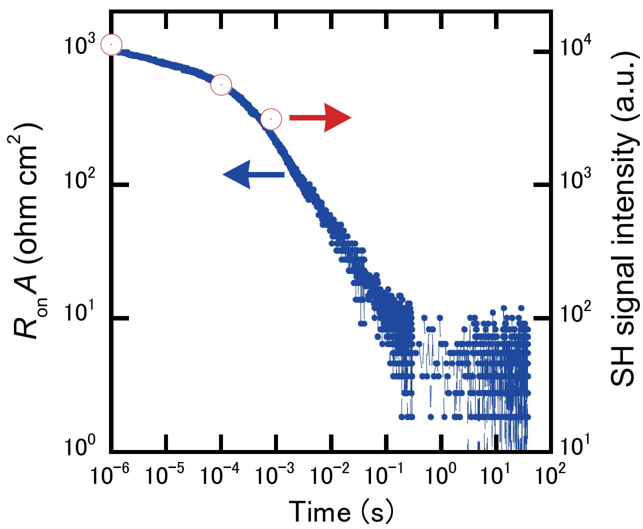

Fig. 6 Time dependence of the SH signal intensity and $R_{on}A$ at the on-state after completion of the applied drain voltage.

300 V under condition (ii). From Figs. 7(b)-(d), it is evident that the SH signals are observed at the gate edge on the drain side, extending from the gate edge in the direction of the drain. The generation of SH signals indicates that the electric field was applied at the depletion layer. Weak SH signals were observed at the left side of Figs. 7(b)-(d), which indicates that there may be insufficient laser irradiation, so that the SH signals are weakened. The SH signals appeared uniformly at the gate edge on the drain side at 100 and 200 V in Figs. 7(b) and (c), respectively, which indicates that the sample was not damaged under this stress condition.

The SH signal intensity at the off-state is clearly larger than that of the on-state, as shown in Fig. 5, although the SH signal distributions for conditions (i) and (ii) are similar. The locations of the highest SH signal intensity for conditions (i) and (ii) correspond with each other, which indicates that the carriers are easily trapped with a high electric field under the off-state. On the other hand, to cause a weak electric field at the off-state is important to reduce the current

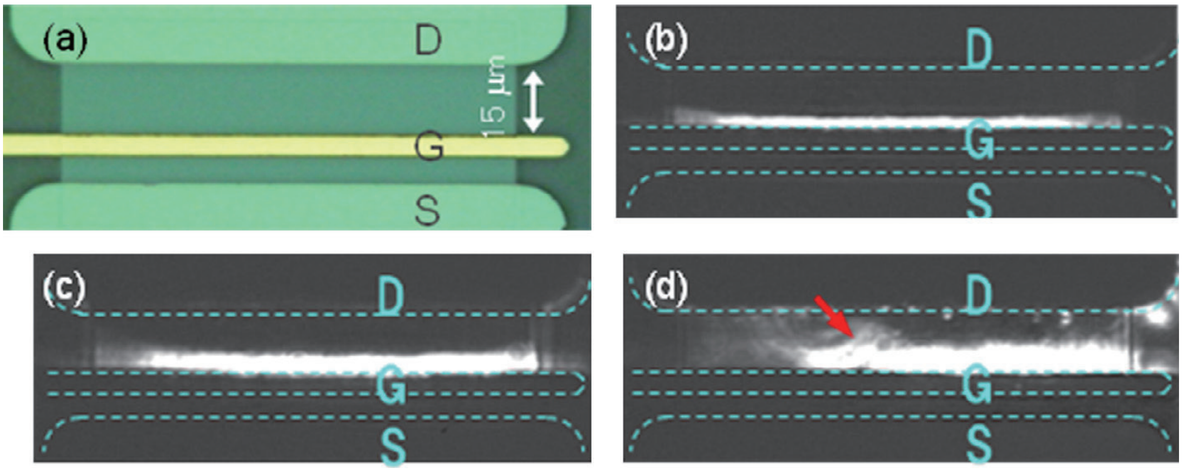

Fig. 7 (a) Optical microscopy images of the AlGaN/GaN HEMT device surface, and (b)-(d) SH signals obtained at drain voltages of 100, 200 and 300 V at the off-state, respectively.

collapse phenomenon. The field plate structure is well known for suppression of the electric field, and has been confirmed as an effective method to reduce the current collapse phenomenon.

The slopes of the SH signal plots in Fig. 5 are almost identical for each of the three voltages,(38) which indicates that the electric field distributions are similar under each condition, with the exception of the region denoted by the red arrow in Fig. 7(d), where non-uniform SH signals from the gate edge are observed. This phenomenon suggests that the electric field is concentrated at this point and thus generates a particularly strong SH signal. On closer examination, a small surface defect was identified at this point, as shown in the optical microscopy image in **Fig. 8**. This feature may be induced by the stress voltage of 300 V.

It was anticipated that a high drain voltage would be applied to the device in the off-state until evidence of device degradation was observed. The change in the surface morphology or oxide particles after stressing of these devices may be observed around the surface defect. It is difficult to determine the mechanism by which the device is degraded, or the associated factors, after the destruction of the device; however, the observation of an enhanced signal at the site of the inadvertent manufacturing defect indicates that EFISHG measurements have potential for the assessment of some of the associated factors. In particular, the measurements performed in this study enabled the assessment of pre-breakdown phenomena, and thus make it possible to reveal the degradation and destruction mechanisms.

Fig. 8 Optical micrograph of the region of the most intense SH signal observed during the EFISHG measurements.

4. Conclusion

The electric field distributions of AlGaN/GaN HEMT devices were imaged on the basis of EFISHG measurements, which enabled an investigation of both the current collapse and degradation. This measurement is useful to acquire current collapse imaging within a short time after the transition from the off-state to the on-state. Immediately after completion of the drain-stress voltage (e.g., 1, 100 and 800 μs) at 200 V in the off-state, the SH signals appeared within 2 μm from the drain electrode. This signal location corresponds well with the virtual gate model of current collapse. The distributions of SH signals in the on- and off-states were similar, and the formation of a weak electric field at the off-state in the device is effective to suppress current collapse. In addition, a strong SH signal was observed at the location of a small defect in the gate edge upon application of a high drain stress voltage, which enables degradation of the HEMT device to be assessed. Therefore, this measurement technique is capable of detecting pre-breakdown phenomenon and enables analysis of the degradation and destruction mechanisms in HEMTs.

References

(1) Wu, Y.-F., Keller, B. P., Fini, P., Pusl, J., Le, M., Nguyen, N. X., Nguyen, C., Widman, D., Keller, S., Denbaars, S. P. and Mishra, U. K., "Short-channel $Al_{0.5}Ga_{0.5}N$/GaN MODFETs with Power Density > 3 W/mm at 18 GHz", *Electron. Lett.*, Vol. 33, No. 20 (1997), pp. 1742-1743.

(2) Sheppard, S. T., Doverspike, K., Pribble, W. L., Allen, S. T., Palmour, J. W., Kehias, L. T. and Jenkins, T. J., "High-power Microwave GaN/AlGaN HEMTs on Semi-insulating Silicon Carbide Substrates", *IEEE Electron Device Lett.*, Vol. 20, No. 4 (1999), pp. 161-163.

(3) Khan, M. A., Shur, M. S., Chen, Q. C. and Kuznia, J. N., "Current/voltage Characteristic Collapse in AlGaN/GaN Heterostructure Insulated Gate Field Effect Transistors at High Drain Bias", *Electron. Lett.*, Vol. 30, No. 25 (1994), pp. 2175-2176.

(4) Klein, P. B., Binari, S. C., Ikossi, K., Wickenden, A. E., Koleske, D. D. and Henry, R. L., "Current Collapse and the Role of Carbon in AlGaN/GaN High Electron Mobility Transistors Grown by Metalorganic Vapor-phase Epitaxy", *Appl. Phys. Lett.*, Vol. 79, No. 21 (2001), pp. 3527-3529.

(5) Hasegawa, H., Inagaki, T., Ootomo, S. and Hashizume, T., "Mechanisms of Current Collapse and Gate Leakage Currents in AlGaN/GaN Heterostructure Field Effect Transistors", *J. Vac. Sci. Technol. B*, Vol. 21, No. 4 (2003), pp. 1844-1855.

(6) Faqir, M., Bouya, M., Malbert, N., Labat, N., Carisetti, D., Lambert, B., Verzellesi, G. and Fantini, F., "Analysis of Current Collapse Effect in AlGaN/GaN HEMT: Experiments and Numerical Simulations", *Microelectron. Reliab.*, Vol. 50, No. 9-11 (2010), pp. 1520-1522.

(7) Makaram, P., Joh, J., del Alamo, J. A., Palacios, T. and Thompson, C. V., "Evolution of Structural Defects Associated with Electrical Degradation in AlGaN/GaN High Electron Mobility Transistors", *Appl. Phys. Lett.*, Vol. 96, No. 23 (2010), 233509.

(8) Tapajna, M., Kaun, S. W., Wong, M., H., Gao, F., Palacios, T., Mishra, U. K., Speck, J. S. and Kuball, M., "Influence of Threading Dislocation Density on Early Degradation in AlGaN/GaN High Electron Mobility Transistors", *Appl. Phys. Lett.*, Vol. 99, No. 22 (2011), 223501.

(9) Joh, J. and del Alamo, J. A., "A Current-transient Methodology for Trap Analysis for GaN High Electron Mobility Transistors", *IEEE Trans. Electron Devices*, Vol. 58, No. 1 (2011), pp. 132-140.

(10) Bisi, D., Meneghini, M., Santi, C. D., Chini, A., Dammann, M., Brückner, P., Mikulla, M., Meneghesso, G. and Zanoni, E., "Deep-level Characterization in GaN HEMTs-Part I: Advantages and Limitations of Drain Current Transient Measurements", *IEEE Trans. Electron Devices*, Vol. 60, No. 10 (2013), pp. 3166-3175.

(11) Meneghini, M., Ronchi, N., Stocco, A., Meneghesso, G., Mishra, U. K., Pei, Y. and Zanoni, E., "Investigation of Trapping and Hot-electron Effects in GaN HEMTs by Means of a Combined Electrooptical Method", *IEEE Trans. Electron Devices*, Vol. 58, No. 9 (2011), pp. 2996-3003.

(12) Huolin, H., Liang, Y. C., Samudra, G. S., Ting-Fu, C. and Chih-Fang, H., "Effects of Gate Field Plates on the Surface State Related Current Collapse in AlGaN/GaN HEMTs", *IEEE Trans. Power Electronics*, Vol. 29, No. 5 (2014), pp. 2164-2173.

(13) Saadaoui, S., Salem, M. M. B., Gassoumi, M., Maaref, H. and Gaquiére, C., "Anomaly and Defects Characterization by I-V and Current Deep Level Transient Spectroscopy of $Al_{0.25}Ga_{0.75}N$/GaN/SiC High Electron-mobility Transistors", *J. Appl. Phys.*, Vol. 111, No. 7 (2012), 073713.

(14) Koley, G., Tilak, V., Eastman, L. F. and Spencer, M. G., "Slow Transients Observed in AlGaN/GaN HFETs: Effects of SiN_x Passivation and UV Illumination", *IEEE Trans. Electron Devices*, Vol. 50, No. 4 (2003), pp. 886-893.

(15) Nakagami, K., Ohno, Y., Kishimoto, S., Maezawa, K., and Mizutani, T., "Surface Potential Measurements of AlGaN/GaN High-electron-mobility Transistors by Kelvin Probe Force Microscopy", *Appl. Phys. Lett.*, Vol. 85, No. 24 (2004), pp. 6028-6029.

(16) Sabuktagin, S., Dogan, S., Baski, A. A. and Morkoç, H., "Surface Charging and Current Collapse in an AlGaN/GaN Heterostructure Field Effect Transistor", *Appl. Phys. Lett.*, Vol. 86, No. 8 (2005), 083506.

(17) DasGupta, S., Biedermann, L., Sun, M., Kaplar, R. J., Marinella, M. J., Zavadil, K., Atcitty, S. and Palacios, T., "Influence of Barrier Design on Current Collapse in High Voltage AlGaN/GaN HEMTs", *IEEE Int. Reliab. Phys. Symp.* (*IRPS*) (2013), pp. 3C.4.1-6.

(18) Delage, S. L. and Dua, C., "Wide Band Gap Semiconductor Reliability: Status and Trends", *Microelectron. Reliab.*, Vol. 43 , No. 9-11 (2003), pp. 1705-1712.

(19) Meneghesso, G., Verzellesi, G., Danesin, F., Rampazzo, F., Zanon, F., Tazzoli, A., Meneghini, M. and Zanoni, E., "Reliability of GaN High-electron-mobility Transistors: State of the Art and Perspectives", *IEEE Trans. Device Mater. Reliab.*, Vol. 8, No. 2 (2008), pp. 332-343.

(20) del Alamo, J. A. and Joh, J., "GaN HEMT Reliability", *Microelectron. Reliab.*, Vol. 49, No. 9-11 (2009), pp. 1200-1206.

(21) Chang, C.-Y., Douglas, E. A., Kim, J., Lu, L., Lo, C. F., Chu, B.-H., Cheney, D. J., Gila, B. P., Ren, F., Via, G. D., Cullen, D. A., Zhou, L., Smith, D. J., Jang, S. and Pearton, S. J., "Electric-field-driven Degradation in OFF-state Step-stressed AlGaN/GaN High-electron Mobility Transistors", *IEEE Trans. Device Mater. Reliab*., Vol. 11, No. 1 (2011), pp. 187-193.
(22) Tapajna, M., Mishra, U. K. and Kuball, M., "Importance of Impurity Diffusion for Early Stage Degradation in AlGaN/GaN High Electron Mobility Transistors upon Electrical Stress", *Appl. Phys. Lett*., Vol. 97, No. 2 (2010), 023503.
(23) Makaram, P., Joh, J., del Alamo, J. A., Palacios, T. and Thompson, C. V., "Evolution of Structural Defects Associated with Electrical Degradation in AlGaN/GaN High Electron Mobility Transistors", *Appl. Phys. Lett*., Vol. 96, No. 23 (2010), 233509.
(24) Gao, F., Lu, B., Li, L., Kaun, S., Speck, J. S., Thompson, C. V. and Palacios, T., "Role of Oxygen in the OFF-state Degradation of AlGaN/GaN High Electron Mobility Transistors", *Appl. Phys. Lett*., Vol. 99, No. 22 (2011), 223506.
(25) Bajo, M. M., Hodges, C., Uren, M. J. and Kuball, M., "On the Link between Electroluminescence, Gate Current Leakage, and Surface Defects in AlGaN/GaN High Electron Mobility Transistors upon Off-state Stress", *Appl. Phys. Lett*., Vol. 101, No. 3 (2012), 033508.
(26) Meneghini, M., Stocco, A., Ronchi, N., Rossi, F., Salviati, G., Meneghesso, G. and Zanoni, E., "Extensive Analysis of the Luminescence Properties of AlGaN/GaN High Electron Mobility Transistors", *Appl. Phys. Lett*., Vol. 97, No. 6 (2010), 063508.
(27) Killat, N., Uren, M. J., Wallis, D. J., Martin, T. and Kuball, M., "Origin of Kink Effect in AlGaN/GaN High Electron Mobility Transistors: Yellow Luminescence and Fe Doping", *Appl. Phys. Lett*., Vol. 101, No. 15 (2012), 153505.
(28) Chang, C.-Y., Anderson, T., Hite, J., Lu, L., Lo, C.-F., Chu, B.-H., Cheney, D. J., Douglas, E. A., Gila, B. P., Ren, F., Via, G. D., Whiting, P., Holzwoeth, R., Jones, K. S., Jang, S. and Pearton, S. J., "Reverse Gate Bias-induced Degradation of AlGaN/GaN High Electron Mobility Transistors", *J. Vac. Sci. Technol. B*, Vol. 28, No. 5 (2010), pp. 1044-1047.
(29) Manaka, T., Lim, E., Tamura, R. and Iwamoto, M., "Modulation in Optical Second Harmonic Generation Signal from Channel of Pentacene Field Effect Transistors during Device Operation", *Appl. Phys. Lett*., Vol. 87, No. 22 (2005), 222107.
(30) Manaka, T., Lim, E., Tamura, R., Yamada, D. and Iwamoto, M., "Probing of the Electric Field Distribution in Organic Field Effect Transistor Channel by Microscopic Second-harmonic Generation", *Appl. Phys. Lett*., Vol. 89, No. 7 (2006), 072113.
(31) Manaka, T., Lim, E., Tamura, R. and Iwamoto, M., "Direct Imaging of Carrier Motion in Organic Transistors by Optical Second-harmonic Generation", *Nature Photonics*, Vol. 1, No. 10 (2007), pp. 581-584.
(32) Katsuno, T., Manaka, T., Ishikawa, T., Ueda, H., Uesugi, T. and Iwamoto, M., "Current Collapse Imaging of Schottky Gate AlGaN/GaN High Electron Mobility Transistors by Electric Field-induced Optical Second-harmonic Generation Measurement", *Appl. Phys. Lett*., Vol. 104 , No. 25 (2014), 252112.
(33) Sun, C.-K., Liang, J.-C., Wang, J.-C., Kao, F.-J., Keller, S., Mack, M. P., Mishra, U. and DenBaars, S. P., "Two-photon Absorption Study of GaN", *Appl. Phys. Lett*., Vol. 76, No. 4 (2000), pp. 439-441.
(34) Coquillat, D., Vecchi, G., Comaschi, C., Malvezzi, A. M., Torres, J. and d'Yerville, M. L. V., "Enhanced Second- and Third-harmonic Generation and Induced Photoluminescence in a Two-dimensional GaN Photonic Crystal", *Appl. Phys. Lett*., Vol. 87, No. 10 (2005), 101106.
(35) Katsuno, T., Kanechika, M., Itoh, K., Nishikawa, K., Uesugi, T. and Kachi, T., "Improvement of Current Collapse by Surface Treatment and Passivation Layer in p-GaN Gate GaN High-electron-mobility Transistors", *Jpn. J. Appl. Phys*., Vol. 52, No. 4S (2013), 04CF08.
(36) Vetury, R., Zhang, N. Q., Keller, S. and Mishra, U. K., "The Impact of Surface States on the DC and RF Characteristics of AlGaN/GaN HFETs", *IEEE Trans. Electron Devices*, Vol. 48, No. 3 (2001), pp. 560-566.
(37) Morardi, M. and Valizadeh, P., "Analytical Modeling of Current Collapse in AlGaN/GaN HFETs According to the Virtual Gate Concept", *IEEE Trans. Device Mater. Reliab*., Vol. 10, No. 2 (2010), pp. 287-294.
(38) Katsuno, T., Manaka, T., Ishikawa, T., Ueda, H., Uesugi, T. and Iwamoto, M., "Degradation Analysis and Current Collapse Imaging of AlGaN/GaN HEMTs by Measurement of Electric Feld-induced Optical Second-harmonic Generation", *Microelectron. Reliab*., Vol. 54, No. 9-10 (2014), pp. 2227-2231.

Text
Partially reprinted from Microelectron. Reliab., Vol. 54, No. 9-10 (2014), pp. 2227-2231, Katsuno, T., Manaka, T., Ishikawa, T., Ueda, H., Uesugi T. and Iwamoto, M., Degradation Analysis and Current Collapse Imaging of AlGaN/GaN HEMTs by Measurement of Electric Field-induced Optical Second-harmonic Generation, © 2012 Elsevier, with permission from Elsevier.

Takashi Katsuno
Research Fields:
- Power Devices
- Reliability

Academic Degree: Ph.D.
Academic Society:
- The Japan Society of Applied Physics

Takaaki Manaka*
Research Fields:
- Organic Electronic Devices
- Nonlinear Optics
- Organic Material Electronics and Optics

Academic Degree: Dr.Eng.
Academic Societies:
- The Japan Society of Applied Physics
- Institute of Electronics, Information and Communication Engineers
- The Institute of Electrical Engineers of Japan

Awards:
- Best Presentation Award, The Institute of Electrical Engineers of Japan, 2001
- The Young Scientists' Prize, The Commendation for Science and Technology by the Minister of Education, Culture, Sports, Science and Technology, 2012

Tsuyoshi Ishikawa
Research Field:
- Power Semiconductor Devices
- Power Electronics

Academic Degree: Dr.Eng.
Academic Societies:
- IEEE
- The Japan Society of Applied Physics

Hiroyuki Ueda
Research Field:
- Development of Compound Semiconductor Power Devices

Academic Society:
- The Japan Society of Applied Physics

Award:
- 30th JSAP Outstanding Paper Award, The Japan Society of Applied Physics, 2008

Tsutomu Uesugi
Research Fields:
- Power Devices
- Compound Semiconductor

Academic Degree: Ph.D.
Academic Societies:
- The Japan Society of Applied Physics
- The Institute of Electrical Engineers of Japan
- IEEE

Award:
- 30th JSAP Outstanding Paper Award, The Japan Society of Applied Physics, 2008

Mitsumasa Iwamoto*
Research Fields:
- Dielectric Physics
- Organic Electronic Materials and Their Properties
- Organic Electronic Devices
- Liquid Crystals

Academic Degree: Dr.Eng.
Academic Societies:
- The Japan Society of Applied Physics
- Institute of Electronics, Information and Communication Engineers
- The Institute of Electrical Engineers of Japan
- The Society of Polymer Science, Japan
- The Surface Science Society of Japan

Awards:
- 13th JSAP Outstanding Paper Award, The Japan Society of Applied Physics, 1991
- Yamazaki Award, The Society of Materials Engineering for Resources of Japan, 1994
- Electronics Society Award , The Institute of Electronics, Information and Communication Engineers, 2001
- Fellow, The Japan Society of Applied Physics, 2010
- Fellow, Information and Communication Engineers, Electronics Society, 2010

* Tokyo Institute of Technology